VERSITA

# THERMAL EFFECTS ON CATHODOLUMINESCENCE IN FORSTERITE

**HIROTSUGU NISHIDO[1], TARO ENDO[1], KIYOTAKA NINAGAWA[2],
MASAHIRO KAYAMA[3] and ARNOLD GUCSIK[4]**

[1]*Department of Biosphere-Geosphere Science, Okayama University of Science,
1-1 Ridaicho, Kita-ku, Okayama, Okayama, 700-0005 Japan*
[2]*Department of Applied Physics, Okayama University of Science,
1-1 Ridaicho, Kita-ku, Okayama, Okayama, 700-0005 Japan*
[3]*Department of Earth and Planetary Systems Science, Graduate School of Science, Hiroshima University,
1-3-1 Kagami-yama, Higashi-Hiroshima, Hiroshima, 739-8526 Japan*
[4]*Department of Earth and Planetary Science, Graduate School of Science, Tohoku University
6-3 Aoba, Aramaki, Aoba, Sendai, 980-8578 Japan*

**Abstract:** Cathodoluminescence (CL) spectral analysis has been conducted for luminescent forsterite (olivine) of terrestrial and meteoritic origins. Two emission bands at 3.15 and 2.99 eV in blue region can be assigned to structural defect centres and two emission bands at 1.91 and 1.74 eV in red region to impurity centres of $Mn^{2+}$ and $Cr^{3+}$, respectively. These emissions reduce their intensities at higher temperature, suggesting a temperature quenching phenomenon. The activation energy in the quenching process was estimated by a least-square fitting of the Arrhenius plots using integrated intensity of each component as follows; blue emissions at 3.15 eV: 0.08-0.10 eV and at 2.99 eV: 0.09-0.11 eV, red emissions at 1.91 eV: ~0.01 eV and at 1.74 eV: ~0.02 eV. The quenching process can be construed by the non-radiative transition by assuming the Mott-Seitz model. The values of activation energies for blue emissions caused by structural defects correspond to the vibration energy of Si–O stretching mode in the lattice, and the values for red emissions caused by Mn and Cr impurity centres to Mg–O vibration energy. It implies that the temperature quenching energy might be transferred as a phonon to the specific lattice vibration.

**Keywords:** forsterite, cathodoluminescence, thermal effect.

## 1. INTRODUCTION

Cathodoluminescence (CL), the emission of visible light caused by electron irradiation, has been extensively applied to geoscience by the reason of high detection sensitivity of emission centre such as impurity elements and various structural defects, because it is very difficult to obtain such valuable information using other analytical methods (e.g., Pagel *et al.*, 2000). The CL method has been used to characterize radiation damage such as CL halo of quartz and feldspar for the application to geodosimetry and furthermore geochronology (e.g. Okumura *et al.*, 2008; Krickl *et al.*, 2008; Kayama *et al.*, 2011), whereas most of radiation-damage in these minerals are not observable with an optical microscope. Recently, the Hayabusa spacecraft successfully recovered dust particles including olivine from the surface of near-Earth asteroid 25143 (Itokawa), which recorded incipient space weath-

Corresponding author: H. Nishido
e-mail: nishido@rins.ous.ac.jp

ering of the surface of airless bodies exposed to the space (Noguchi *et al.*, 2011). Micro-CL analysis using a scanning electron microscope-cathodoluminescence (SEM-CL) with a high spatial resolution could detect ultrathin layer of space weathering on the surface of olivine particle caused by high-energy cosmic radiation.

Olivine, a magnesium iron silicate with the formula $(Mg,Fe)_2SiO_4$, is one of the important minerals constituting the terrestrial planets as well as almost chondritic meteorites in the solar system. CL spectral analysis provides valuable information on a combination of various activators and defect centres in olivine. Forsterite, near Mg-end member of olivine, in meteorites occasionally shows luminescence, whereas terrestrial one mostly gives no luminescence. CL zoning of the forsterite in carbonaceous meteorites has been investigated to clarify the origin and thermal history of the chondrules. In this case, small amount of divalent Fe ions as quencher easily eliminate CL emissions caused by impurity and defect centres, so only near-end forsterite can show CL emissions. Such environmental condition should be limited to be in the process of primary stage of chondrule formation or subsequent reductive stage occasionally with low $fo_2$ aqueous alteration (Brearley and Jones, 1998) rather than terrestrial condition. Recently CL microcharacterization of laboratory forsterite chondrules has shown to provide valuable information on the formation process and related mechanism of the crystal growth in a supercooled melt, resulting in clear assignments of luminescence centres in forsterite including a microdefect-related centre due to a rapid crystal growth (Gucsik *et al.*, 2012).

The factors affect the CL in forsterite, e.g.: luminescence centres, have been investigated considerably, however, the temperature effect on CL efficiency has not been discussed despite its potentially important function to control CL emission mechanism. In this study we have characterized various types of luminescence centres derived from the forsterite in a wide range of temperature using a SEM-CL, and confirmed temperature quenching of their emissions. The quenching process has been quantitatively evaluated by CL spectral deconvolution method assuming the Mott-Seitz model.

## 2. SAMPLES AND EXPERIMENTAL

A clear transparent crystal of forsterite (Fo:99.1) in basalt from Mogok, Myanmar and micro-grains of forsterite (Fo:99.7-99.8) in chondrules from Allende and Kaba meteorites classified as a CV3 carbonaceous chondrite were prepared for CL spectral measurements. The polished samples were fixed on a slide glass with epoxy resin (I.T.W. industry: Devcon ET), which shows almost no luminescence, was coated with ~2 nm carbon thin-film to prevent a charging up on the surface.

CL spectroscopy was made by a SEM-CL system, which is comprised of SEM (JEOL: JSM-5410LV) combined with a grating monochromator (OXFORD: Mono

CL2). The CL emitted from the samples was collected using a retractable parabolic mirror coated with aluminium (collecting efficiency of 75%). The CL was dispersed by a grating monochromator, which has the following characteristics: 1200 grooves/mm, a focal length of 0.3 m, F of 4.2, limit of resolution of 0.5 nm, and slit width of 4 mm at the inlet and outlet. The dispersed CL was recorded by a photon counting method using a photomultiplier tube (Hamamatsu: R2228) and converted to digital data. The CL spectral measurements were carried out at various temperatures ranging from −190 to 0°C. The sample temperature was controlled by liquid nitrogen and embedded heater in a cryostage (Oxford: C1003).

All CL spectra were corrected for total instrumental response, which was determined using a calibrated standard lamp (Eppley Laboratory: Quartz Halogen Lamp). This correction prevents errors in the peak position of emission bands and allows quantitative evaluation of CL intensity. The spectral response varies smoothly between 300 and 800 nm with a maximum at 550 nm and shows the steps at approximately 450 and 730 nm, which correspond to discontinuous artifacts of Wood's anomaly attributed to a specific characteristic of the grating. Detailed construction of the equipment and analytical procedure can be followed from Ikenaga *et al.* (2000). The corrected CL spectra in energy unit were deconvoluted into the Gaussian component corresponding to each emission centre using a peak-fitting software (Peak Analyzer) in OriginPro 8J SR2.

## 3. RESULTS AND DISCUSSION

At room temperature, the CL spectra of all samples show broad emission bands at around 400 nm in blue region and at around 650 nm in red region, and a broad emission band close to IR region at around 750 nm (**Fig. 1**). According to previous works on forsterite CL (e.g. Steele *et al.*, 1985; Benstock *et al.*, 1997), the blue emission could be assigned to the defect centre (intrinsic de-
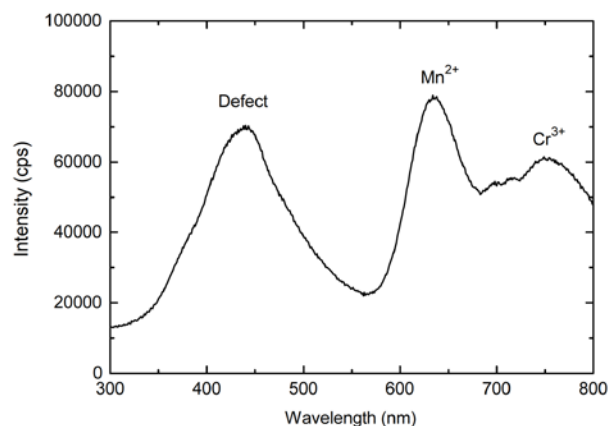


**Fig. 1.** *CL spectrum of forsterite in chondrule (Allende meteorite).*

fect) related to lattice defects associated with $Al^{3+}$ substitution for $Si^{4+}$, or deformation of the lattice due to an incorporation of Ca and Ti ions. The red emission band at around 650 nm is assigned to $Mn^{2+}$ impurity centre in an octahedral coordination and preferred in the M2 site, which was observed in meteoritic forsterite samples as well as in Mn-doped synthetic samples (McCormick *et al.*, 1987; Benstock *et al.*, 1997). The red-IR emission band at around 720 nm might be attributed to $Cr^{3+}$ in the M1 and/or M2 site, which acts as an activator and possibly associated with structural defect caused by interstitial Cr ions in IR region, according to the result of CL spectroscopy for Cr-doped forsterite (Moncorgé *et al.*, 1991; Benstock *et al.*, 1997).

Their emission intensities decrease with an increase in sample temperature. The peak positions of the red emissions at around 650 and 720 nm are slightly shifted to shorter wavelengths ($\Delta\lambda \sim 5$ nm) with an increasing temperature whereas the peak positions of the blue emission are independent on the sample temperature. The peak wavelength of the emission activated by transition metal elements such as Mn and Cr is closely related to the crystal-field strength particularly depending on metal-ligand distance (Burns, 1993). Therefore, it should be usually controlled by thermal vibration in the lattice, but this is not in the case for the emission band caused by defect centre.

In general, the luminescence efficiency of the material decreases with a rise in temperature due to an increase in non-radiative transitions. This phenomenon has been recognized in several minerals such as quartz, cristobalite and tridymite as temperature quenching (Hanusiak and White, 1975; Luff and Townsend, 1990; Stevens-Kalceff *et al.*, 2000; Kayama *et al.*, 2009). The luminescent efficiency ($\eta$) is well represented by the following equation (Curie, 1963; Yacobi and Holt, 1990), where A is for a probability of radiative transition, s for frequency factor, k for Boltzmann constant, T for absolute temperature and $\varepsilon$ for activation energy.

$$\eta = \frac{A}{A + s \exp\left(-\dfrac{\varepsilon}{kT}\right)} \tag{3.1}$$

The activation energy (eV) is assumed by the Mott-Seitz model for temperature quenching of luminescence derived from the theory proposed by Mott and Gurney (1948) and Seitz (1939), assuming an increase in the probability of a non-radiative transition with increasing sample temperature. In this case, a probability of radiative transition (A) is independent upon sample temperature, and is regarded as constant in the equation. The luminescent efficiency ($\eta$) can be estimated from the integrated intensity calculated by a Gaussian fit to the CL emission components. According to Steven-Kalceff (2009) and Kayama *et al.* (2010), the CL spectra in energy units can be successfully deconvoluted into four

Gaussian-fitted components corresponding to two defect centres and two impurity centres using a peak-fitting software in OriginPro 8 (**Fig. 2**), where the number of the components was determined on the basis of a statistical test of $\chi^2$ factor proposed by Stevens-Kalceff (2009).

The emission peak in the blue region can be separated into two components centred at 3.15 (defect 1) and at 2.99 eV (defect 2), and the peaks in the red region into two components centred at 1.91 ($Mn^{2+}$) and 1.74 eV ($Cr^{3+}$). By assuming the Mott-Seitz model, activation energy in each temperature quenching process can be calculated by a plot of $\ln[(1/\eta)-1]$ against $1/T$ (Arrhenius plot) using integrated intensity of each component. The straight-line relationship for each emission component is recognized in the plots (**Fig. 3**), which can be clearly explained on the basis of Mott-Seitz theory. The emission of all samples show a similar behaviour of CL quenching on heating, and the slopes of two defect components are relatively higher than those of two impurity components. Each activation energy was determined as follows; blue emission (defect 1) at 3.15 eV: 0.08-0.10 eV, blue emission (defect 2) at 2.99 eV: 0.09-0.11 eV, red emission ($Mn^{2+}$) at 1.91 eV: ~0.01 eV, red emission ($Cr^{3+}$) at 1.74 eV: ~0.02 eV.

The vibration energies of forsterite can be obtained from Raman and IR spectroscopy data (Hofmeister, 1987: Chopelas, 1991; Mouri and Enami, 2008). The energy value of 0.08-0.11 eV (445-888 $cm^{-1}$) for defect centres corresponds to that of Si-O stretching vibrations in forsterite lattice and the value of 0.01-0.02 eV (81-162 $cm^{-1}$) for impurity centres possibly to the vibration energy of M-O bond. Therefore, the activation energy in the temperature quenching process for each luminescent centre in forsterite could be assigned to specific lattice motions. Judging from the similarity of the activation energy in the process of temperature quenching and lattice vibration energy, the temperature quenching energy might be transferred as a phonon to the specific lattice vibration through
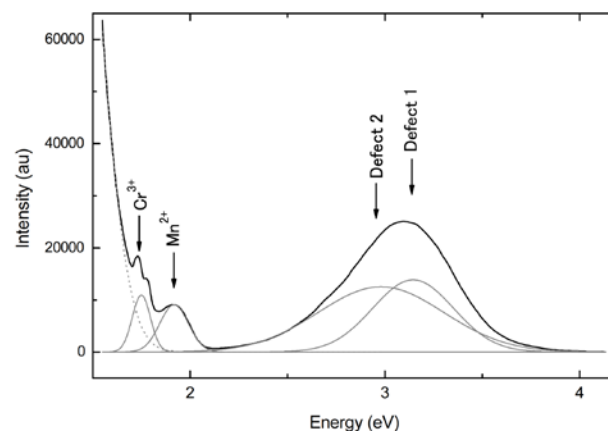


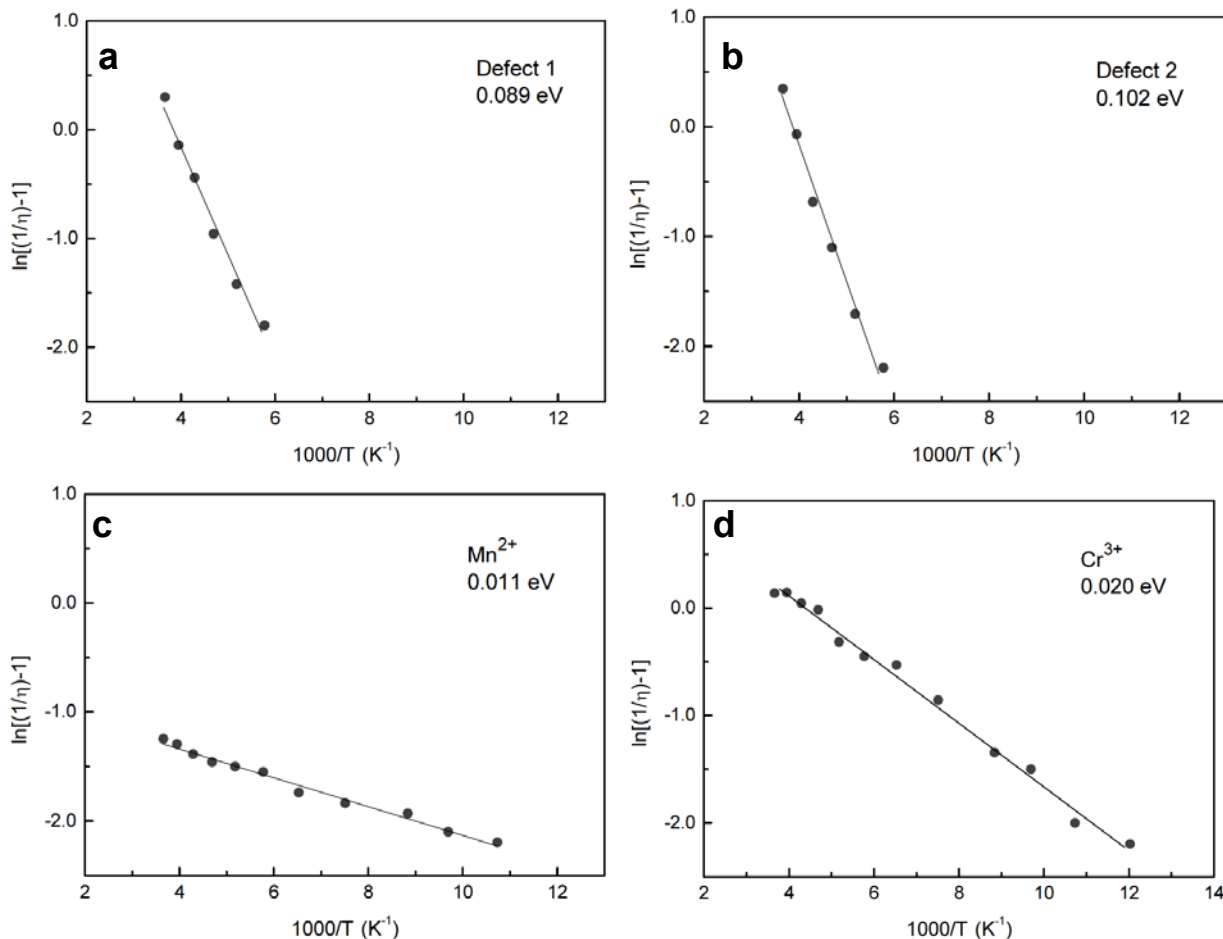**Fig. 2.** *Spectral deconvolution of forsterite CL in chondrule (Allende meteorite) by Gaussian fitting.*

**Fig. 3.** *Arrhenius plots of ln [1/η−1] against 1000/T for each emission of Allende forsterite. a: emission component at 3.15 (defect 1), b: emission component at 2.99 (defect 2), c: emission component at 1.91 (Mn$^{2+}$), d: emission component at 1.74 (Cr$^{3+}$).*

non-radiative transition. Kayama *et al.* (2009) clarified the process of temperature quenching in the CL of tridymite and cristobalite, and estimated that Si-O stretching vibration energy is 0.03-0.14 eV (1049-1130 cm$^{-1}$) for tridymite and 0.15-0.16 eV (1211-1249 cm$^{-1}$) for cristobalite. The corresponding emissions are identified as short-lived blue luminescence derived from the defect closely associated with Al$^{3+}$ impurity substituting Si$^{4+}$ in the Si-O tetrahedra. In crystal structure of forsterite, three different lengths of Si-O bond are recognized (Deer *et al.*, 1982), suggesting various types of tetrahedra with slightly modified coordination with surrounding cations. It implies that two types of defect centres (defect 1 and 2) might be due to different types of tetrahedra caused by Al$^{3+}$ impurity substitution.

Forsterite is a key mineral to solve many problems in geoscientific fields because it is one of the most abundant and widespread minerals in the earth-type planets and asteroids. In particular we could find luminescent forsterite from a great number of meteorites, and furthermore we were able to obtain raw materials including forsterite

of asteroids by the Sample Return Project (e.g. Hayabusa II Project to be planned in Japan). Recently the luminescence investigation of forsterite has been done for a better understanding of radiogenic damage processes in forsterite related to cosmic weathering and its extreme environmental conditions such as rapid growth at ~10 mm/s or high from a supercooled melt (Gucsik *et al.* 2012). Temperature quenching of CL is an important factor to control the emission efficiency of forsterite, so our results would be expected to contribute as valuable information on forsterite CL, especially for quantitative estimation of radiation dose (CL dosimetry) irradiated on the forsterite in cosmic space.

## ACKNOWLEDGEMENTS

# REFERENCES

Benstock EJ, Buseck PR and Steele IM, 1997. Cathodoluminescence of meteoritic and synthetic forsterite at 296 and 77 K using TEM. *American Mineralogist* 82: 310-315.

Brearley AJ and Jones RH, 1998. Chondritic meteorites, Planetary Materials. *Reviews in mineralogy* 36: 3-01-370.

Burns RG, 1993. Mineralogical Applications of Crystal Field Theory. 2nd edition, Cambridge University Press.7-43.

Chopelas A, 1991. Single crystal Raman spectra of forsterite, fayalite, and monticellite. *American Mineralogist* 76: 1101-1109.

Curie D, 1963. Thermal and optical activation of trapped electrons: Quenching effects. Luminescence in Crystals. Methuem and Co. Ltd. London. 202-208.

Deer WA, Howie RA and Zussman J, 1982. Rock-Forming Minerals, Volume 1A, Orthosilicates. Longman, London. 4-18.

Gucsik A, Tsukamoto K, Nishido H, Miura H, Kayama M, Ninagawa K and Kimura Y, 2012. Cathodoluminescence microcharacterization of forsterite in the chondrule experimentally under super cooling. *Journal of Luminescence* 132(4): 1041-1047, DOI 10.1016/j.jlumin.2011.12.011.

Hanusiak WM and White EW, 1975. SEM cathodoluminescence for characterization of damaged and undamaged quartz in respirable dusts, Proceeding of the 8th annual scanning electron microscope symposium, III: 125-132.

Hofmeister AM, 1987. Single-crystal absorption and reflection infrared spectroscopy of forsterite and fayalite. *Physics and Chemistry of Minerals* 14(6): 499-513, DOI 10.1007/BF00308285.

Ikenaga M, Nishido H and Ninagawa K, 2000. Performance and analytical conditions of cathodoluminescence scanning electron microscope (CL-SEM). *Bulletin of Research Institute of Natural Sciences Okayama University of Science* 26: 61-75.

Kayama M, Nishido H and Ninagawa K, 2009. Cathodoluminescence characterization of tridymite and cristobalite: Effects of electron irradiation and sample temperature. *American Mineralogist* 94: 1018-1028.

Kayama M, Nakano S and Nishido H, 2010. Characteristics of emission centres in alkali feldspar: A new approach by using cathodoluminescence spectral deconvolution. *American Mineralogist* 95: 1783-1795.

Kayama M, Nishido H and Ninagawa K, 2011. Radiation effects on cathodoluminescence of albite. *American Mineralogist* 96: 1238-1247.

Krickl R, Nasdala L, Götze J, Grambole D and Wirth R, 2008. Alpha-irradiation effects in $SiO_2$. *European Journal of Mineralogy* 20: 517-522, DOI 10.1127/0935-1221/2008/0020-1842.

Luff B and Townsend P, 1990. Cathodoluminescence of synthetic quartz. *Journal of Physics: Condensed Matter* 2(40): 8089-8097, DOI 10.1088/0953-8984/2/40/009.

McCormick TC, Smyth JR and Lofgren GE, 1987. Site occupancies of minor elements in synthetic olivines as determined by channeling enhanced X-ray emission. *Physics and Chemistry of Minerals* 14(4): 368-372, DOI 10.1007/BF00309812.

Moncorgé R, Cormier G, Simkin DJ and Capobianco JA, 1991. Fluorescence analysis of chromium-doped forsterite ($Mg_2SiO_4$). *Journal of Quantum Electronics* 27(1): 114-120, DOI 10.1109/3.73548.

Mott NF and Gurney RW, 1948. Electronic Processes in Ionic Crystals. Clarendon Press, Oxford. 219-224.

Mouri T and Enami M, 2008. Raman spectroscopic study of olivine-group minerals. *Journal of Mineralogical and Petrological Sciences* 103(2): 100-104, DOI 10.2465/jmps.071015.

Noguchi T, Nakamura T, Kimura M, Zolensky ME, Tanaka M, Hashimoto T, Konno M, Nakato A, Ogami T, Fujimura A, Abe M, Yada T, Mukai T, Ueno M, Okada T, Shirai K, Ishibashi Y and OkazakiR, 2011. Incipient space weathering observed on the surface of Itokawa dust particles. *Science* 333: 1121-1125, DOI 10.1126/science.1207794.

Okumura T, Nishido H, Toyoda S, Kaneko T, Kosugi S and Sawada Y, 2008. Evaluation of radiation-damage halos in quartz by cathodoluminescence as a geochronological tool. *Quaternary Geochronology* 3(4): 342-345, DOI 10.1016/j.quageo.2008.01.006.

Pagel M, Barbin V, Blanc P and Ohnenstetter D (eds.), 2000. Cathodoluminescence in Geoscience. Springer-Verlag. 1-514.

Seitz F, 1939. An introduction of crystal luminescence. *Transactions of the Faraday Society* 35: 74-85, DOI 10.1039/TF9393500074.

Steele IM, Smith JV and Sirikus C, 1985. Cathodoluminescence zoning and minor elements in forsterites from the Murchison (C2) and Allende (C3V) carbonaceous chondrites. *Nature* 313(6000): 294-297, DOI 10.1038/313294a0.

Stevens-Kalceff MA, 2009. Cathodoluminescence microcharacterization of point defect in α-quartz. *Mineralogical Magazine* 73: 585-605, DOI 10.1180/minmag.2009.073.4.585.

Stevens-Kalceff MA, Matthew RP, Anthony RM and Kalceff W, 2000. Cathodoluminescence microcharacterisation of silicon dioxide polymorphs. Cathodoluminescence in Geosciences. Springer, Berlin, 8: 193-223.

Yacobi BG and Holt DB, 1990. Cathodoluminescence Microscopy of Inorganic Solids. Plenum Press, New York. 21-54.